Devices

Mater. Res. Soc. Symp. Proc. Vol. 957 © 2007 Materials Research Society 0957-K01-05

Development of Thin Film and Nanorod ZnO-Based LEDs and Sensors

S. J. Pearton[1], L. C. Tien[1], H. S. Kim[1], D. P. Norton[1], J. J. Chen[2], H. T. Wang[2], B. S. Kang[2], F. Ren[2], W. T. Lim[1], J. Wright[1], R. Khanna[1], L. F. Voss[1], L. Stafford[1], J. Jun[3], and Jenshan Lin[3]
[1]MSE, University of Florida, Gainesville, FL, 32611
[2]Chemical Engineering, University of Florida, Gainesville, FL, 32611
[3]ECE, University of Florida, Gainesville, FL, 32611

ABSTRACT

The development of new etching and contact metallurgies for the ZnO/ZnMgO/ZnCdO materials system and various approaches for realizing ZnO LEDs are reviewed. ZnO nanorod MOSFETs and pH sensors have been demonstrated. In addition, selective detection of hydrogen with Pt-coated single ZnO nanorods is discussed discussed. The Pt-coated single nanorods show a current response approximately a factor of three larger at room temperature upon exposure to 500ppm H_2 in N_2 than thin films of ZnO. The power consumption of these sensors can be very small (in the nW range) when using discontinuous coatings of Pt. Once the Pt coating becomes continuous, the current required to operate the sensors increases to the μW range. The ZnO nanorods are insensitive to oxygen in the measurement ambient.

INTRODUCTION

ZnO is attracting attention for transparent electronics, sensors and UV light emitters. ZnO has the advantage of a relative low growth temperature which is suitable for deposition on cheap glass substrates and much higher excition binding energy (~ 60meV) than GaN (25meV). The excitons in the ZnO semiconductor will not dissociate into free electrons or holes due to the heat at room temperature or the scattering between the excitons. Additionally, commercial ZnO substrates are available. The ZnO system also has a simpler processing relative to GaN which cannot be wet-etched in conventional acid mixtures at safe temperatures. The curvature of conduction band and valence band for ZnO is smaller than GaN, meaning that the electron effective mass in ZnO will be larger. Some groups have published N-doped or P-doped ZnO-based p-n junction or MIS LEDs[1-14]. Tsukazaki et al, studied ZnO p-i-n homojunction structure on (0001) $ScAlMgO_4$ grown by laser MBE [2,3]. Lim et al. have made p-n homojunction ZnO LED on sapphire by r-f sputtering[5]. Jiao et al. have demonstrated ZnO p-n junction LED on a-plane Al_2O_3 substrate by plasma-assisted MBE [8]. However, much more work is needed on all aspects of ZnO device and materials technology.

In this paper we describe recent progress in developing processes for improved ZnO LEDs and also on development of ZnO nanowire devices.

RESULTS AND DISCUSSION

(i) Contacts

To improve ZnO LED device performance, the development of low resistance Ohmic contacts to ZnO is essential. The conventional contact formation involves the deposition of metal contact on ZnO followed by annealing at elevated temperatures. Some groups have found

low contact resistivity for N-type and P-type ZnO on the order of 10^{-7} and 10^{-5} Ω-cm^2, respectively [15-33].

We summarize some of our recent work as follows:

(a) Ti/Au and Ti/Al/Pt/Au contacts showed specific contact resistivity in the range 1.6-2.3×10^{-4} Ω-cm^2 on lightly n-type ZnCdO layers after annealing at 450-500ºC. The temperature dependence of the specific contact resistivity indicates that the dominant mechanism of current transport is field emission. The creation of oxygen vacancies (V_o) appears to play an important role in the Ohmic nature of the Ti/Au and Ti/Al/Pt/Au contacts through a local increase in electron concentration. The Ti/Au scheme shows superior thermal stability compared to Ti/Al/Pt/Au.

(b) Ohmic contacts using Ti/Au on Al-doped ZnO had the following properties. Contacts made to heavily Al-doped ZnO with carrier concentrations near 10^{19} cm^{-3} show minimum specific contact resistivity of 6.0 ×10^{-8} Ω-cm^2 after annealing at 300ºC(Figure 1). These contacts are Ohmic as-deposited, exhibiting very good specific contact resistances of 2.4x10^{-7} Ω-cm^2. The dominant mechanism of current transport is tunneling, even in the as-deposited contacts, showing the advantage of specifically doping the ZnO.

(c) ITO/Ti/Al contact stacks grown on ZnO produce a contact with a resistance <10^{-5} Ω-cm^2 over a broad range of annealing temperatures and maintains smooth morphology up to 350°C. The ITO refractive index is between that of ZnO and air, which reduces the reflection at the ZnO/air interface. This approach looks promising as a transparent conducting current spreading layer on ZnO-based LEDs.

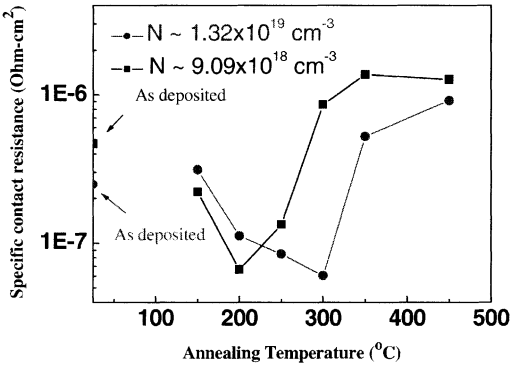

Figure 1. Sheet resistance (top) and transfer resistance (bottom) as a function of annealing temperature for Ti/Au contacts on ZnO:Al.

(ii)Wet Etching

In most device fabrication schemes, wet etching is needed for isolation or mesa formation if nonconductive substrates are used. The binary ZnO is readily etched in many acid solutions, including HNO_3/HCl and HF. In most cases, the etching is reaction limited, with typical thermal activation energies of >6 kCal·mol^{-1}. In preliminary work, we have found that the etching of the ZnO is strongly dependent on material quality. If the ZnO is very thin, the wet etch rates are high in all acid solutions. A particular problem encountered with the wet etching of ZnO/AlGaN-based LED structures was the presence of a very significant undercut (as much as

around 10 μm), which occurred mainly at the end of the selective removal of the ZnO from the underlying AlGaN. There are no reports to date on the wet etching of ZnCdO and ZnMgO and in particular it is important to develop selective etches for ZnCdO/ZnO and ZnMgO/ZnO systems. We demonstrated the achievement of selective etching of ZnCdO over ZnO using both dilute HCl and H_3PO_4 mixtures. We also reported on the selective etching of $Zn_{0.9}Mg_{0.1}O$ relative to ZnO, both grown with similar thicknesses on sapphire substrates by pulsed laser deposition (PLD) to ensure similar crystal quality. In $Zn_{0.9}Mg_{0.1}O$/ZnO system, wet etch selectivities over 400 for ZnMgO over ZnO can be achieved with HCl at high dilution factors with water. ZnCdO, ZnMgO, and ZnO can be readily etched in dilute solutions of HCl and H_3PO_4. High dilution factors of these acids with water provides controllable etch rates in the range 30–90 $nm \cdot min^{-1}$ for ZnCdO and 120–1100 $nm \cdot min^{-1}$ for ZnMgO, with adequate selectivity to ZnO grown under the same conditions, as shown for ZnMgO and ZnO in Figure 2. Photoresist provides a stable and convenient mask for patterning ZnCdO, ZnMgO, and ZnO in these acid solutions. The availability of simple wet solutions for this heterostructure system simplifies the processing of mesa-type ZnO-based LEDs and avoids the need for plasma etching processes which are known to damage the ZnO surface even at low plasma powers.

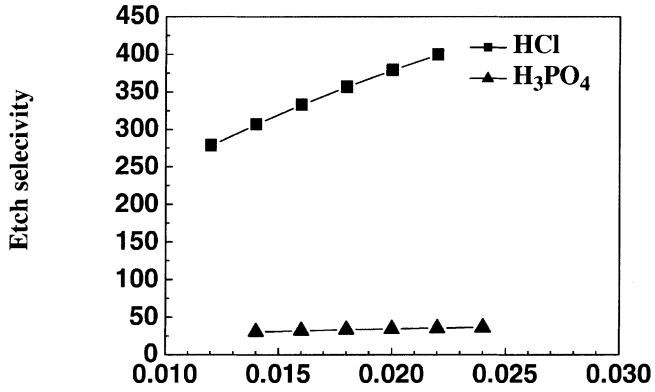

Figure 2. Etch selectivity of ZnMgO to ZnO at room temperature as a function of solution concentration

(iii) ZnO-based Nanowires

Recent experiments in our laboratory varied conditions during nanowire growth to achieve ZnO based nanowire growth with both radial and axial composition variation. These are shown schematically in Figure 3. Axial heterostructures vary in composition along the nanowire growth axis with alternating layers of ZnO and $(Z_{1-x}Mg_x)O$. The two types of axial heterostructures have been grown and evaluated by high resolution TEM, selective area diffraction, STEM, and photoluminescence. In the Type I structure a Zn rich core of wurtzite $(Z_{1-x}Mg_x)O$ is surrounded by a wurtzite $(Z_{1-x}Mg_x)O$ Mg-rich sheath. The second (Type II), grown at a higher Mg pressure, has a wurtzite core with rock-salt sheath surrounding it. UV response of

these heterostructure nanowires has not been evaluated, but the ability to confine carriers in radial and axial directions presents interesting possibilities for tailoring of UV detector properties.

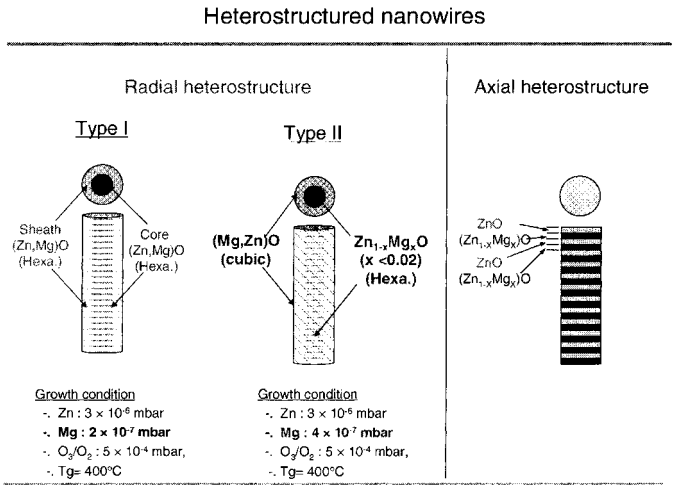

Figure 3. Schematic diagram of nanowires with radial and axial heterostructure.

A summary of the nanowires grown as a function of Mg pressure are shown in Figure 4. These range from wurtzite ZnO (no Mg) nanowires through the two radial structures (Type I, Type II) with increasing pressure, with a cubic rocksalt structure at the maximum pressure 8×10^{-7} mbar.

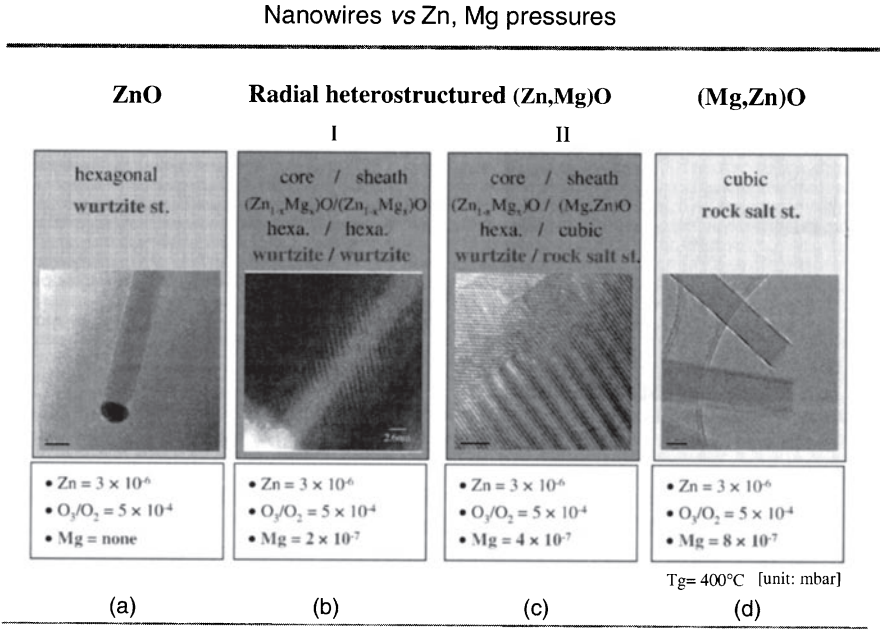

Figure 4. Summary of (ZnMg)O nanowires grown at 400C with varying Mg pressures. STEM results in (a) and (d) show structures for ZnO wurtzite and (Mg,Zn)O rocksalt nanowires, respectively. A high resolution Z-STEM of Type I structure in (b) shows a higher cation mass in the center, indicating Zn rich core. HRTEM in (c) for a Type II structure shows the structure changes from hexagonal to cubic from the nanowire core to the sheath.

(iv) ZnO Nanowire Devices

We have fabricated many types of ZnO nanowire devices, including MOSFETs, diodes, UV sensors and pH sensors. ZnO has been effectively used as a gas sensor material based on the near-surface modification of charge distribution with surface-absorbed species. It is attractive for biosensors given that Zn and Mg are essential elements for neurotransmitter production and enzyme functioning. The large surface area of the nanorods makes them attractive for gas and chemical sensing, and the ability to control their nucleation sites makes them candidates for high density sensor arrays. The sensing mechanism for chemical adsorbates in piezoelectric materials originates from compensation of the polarization -induced bound surface charge by interaction with the polar molecules in the liquids.

Single ZnO nanowire metal-oxide semiconductor field effect transistors (MOSFETs) were fabricated using nanowires grown by site selective MBE. When measured in the dark at 25°C,the depletion-mode transistors exhibit good saturation behavior, a threshold voltage of ~-3V and a maximum transconductance of order 0.3 mS/mm(Figure 5). Under UV (366nm) illumination, the drain-source current increase by approximately a factor of 5 and the maximum transconductance

is ~ 5 mS/mm. The channel mobility is estimated to be ~3 cm^2/V.s, which is comparable to that reported for thin film ZnO enhancement mode MOSFETs and the on/off ratio was ~25 in the dark and ~125 under UV illumination

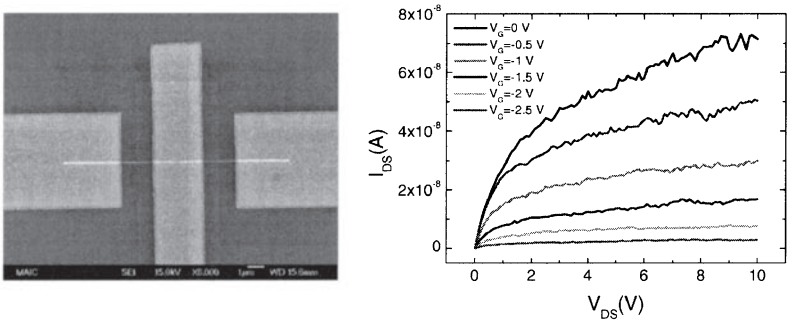

Figure 5. SEM micrograph of fabricated FET. I_{DS}-V_{DS} (top) and transfer characteristics (bottom) of ZnO nanowire FET at room temperature in the dark.

Single ZnO nanorods with Ohmic contacts at either end exhibit large changes in current upon exposing the surface region to polar liquids introduced through an integrated microchannel .The polar nature of the electrolyte introduced led to a change of surface charges on the nanorod, producing a change in surface potential at the semiconductor /liquid interface. The nanorods exhibit a linear change in conductance between pH 2- 12 of 8.5nS/pH in the dark and 20nS/pH when illuminated with UV(365nm) light .The nanorods show stable operation with a resolution of ~0.1 pH over the entire pH range. The results indicate that ZnO nanorods may have application in integrated chemical, gas and fluid monitoring sensors. The pH solution was applied using a syringe autopipette (2-20ul). An SEM of the completed device is shown in Figure 6 (left).

Prior to the pH measurements, we used pH 4, 7, 10 buffer solutions from Fisher Scientific to calibrate the electrode and the measurements at 25 °C were carried out in the dark or under UV illumination from 365 nm light using an Agilent 4156C parameter analyzer to avoid parasitic effects. The pH solution made by the titration method using HNO_3, NaOH and distilled water. The electrode was a conventional Acumet standard Ag/AgCl electrode. The adsorption of polar molecules on the surface of ZnO affects the surface potential and device characteristics. Figure 6 also shows the conductance at a bias of 0.5V as a function of time from nanorods exposed for 60s to a series of solutions whose pH was varied from 2- 12.The current is significantly reduced upon exposure to these polar liquids as the pH is increased. The data in Figure 6 shows that the nanowire sensor is sensitive to the concentration of the polar liquid and therefore could be used to differentiate between liquids into which a small amount of leakage of another substance has occurred. The nanorods exhibited a linear change in conductance between pH 2-12 of 8.5nS/pH in the dark and 20nS/pH when illuminated with UV (365nm) light .The nanorods show stable operation with a resolution of ~0.1 pH over the entire pH range, showing the remarkable sensitivity of the HEMT to relatively small changes in concentration of the liquid.

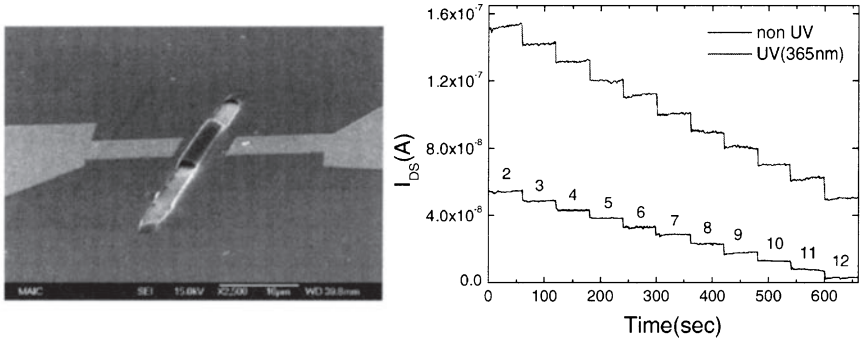

Figure 6. SEM of ZnO nanorod with integrated microchannel (4μm width) and change in current (top) or conductance (bottom) with pH (from 2-12) at V = 0.5V.

We have also been able to use single and multiple nanorods as sensitive hydrogen gas sensors. The use of thin Pt coatings on the nanorods greatly enhances their sensitivity to hydrogen at room temperature. There is currently great interest in the development of hydrogen sensors for applications involving leak detection in hydrogen fuel storage systems and fuel cells for space craft. One of the main demands for such sensors is the ability to selectively detect hydrogen at room temperature in the presence of air. In addition, for most of these applications, the sensors should have very low power requirements and minimal weight. One important aspect is to increase their sensitivity for detecting gases such as hydrogen at low concentrations or temperatures, since typically an on-chip heater is used to increase the dissociation efficiency of molecular hydrogen to the atomic form and this adds complexity and power requirements.

Different metal coating layers on multiple ZnO nanorods were compared for enhancing the sensitivity to detection of hydrogen at room temperature. Pt is found to be the most effective catalyst, followed by Pd. The resulting sensors(shown schematically in Figure 7) are shown to be capable of detecting hydrogen in the range of ppm at room temperature using very small current and voltage requirements and recover quickly after the source of hydrogen is removed. Figure 7 also shows the time dependence of relative resistance change of either metal-coated or uncoated multiple ZnO nanorods as the gas ambient is switched from N_2 to 500 ppm of H_2 in air and then back to N_2 as time proceeds. These were measured a bias voltage of 0.5V. The first point of note is that there is a strong increase (approximately a factor of 5) in the response of the Pt-coated nanorods to hydrogen relative to the uncoated devices. Under these conditions, the resistance response is 8% and is achieved for a power requirement of only 0.4mW.

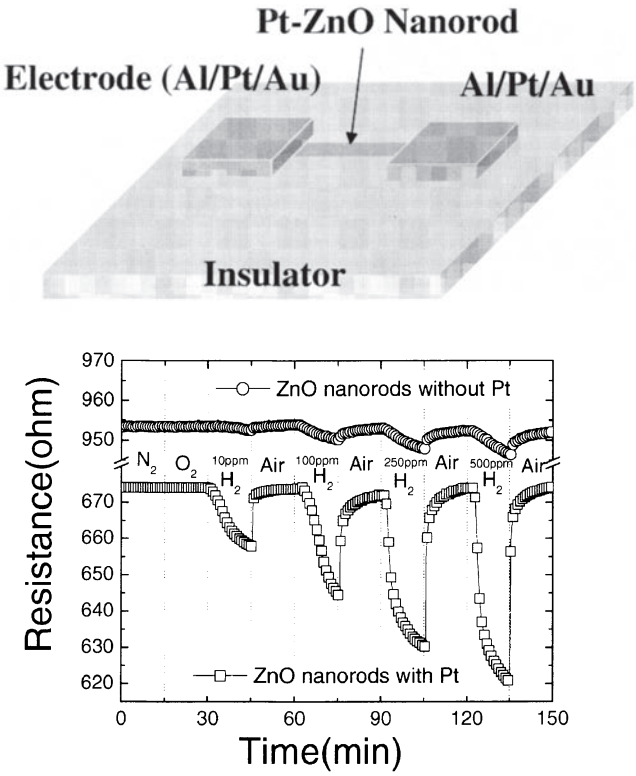

Figure 7. Schematic of ZnO nanorod hydrogen sensor (top) and time dependence of resistance change of either Pt-coated or uncoated multiple ZnO nanowires as the gas ambient is switched from N_2 to oxygen or various concentrations of H_2 in N_2 (10-500 ppm), then to air for recovery.

(v) ZnO UV LEDs using ion implanted ZnO

The samples were (0001) undoped grade I quality bulk, single- crystal ZnO crystals from Cermet. They were epiready with one-side-Zn-face-polished by the manufacturer. The room temperature electron concentration and mobility established by van der Pauw measurements were 10^{17} cm^{-3} and 190 cm^2/V s, respectively. Ion implantation was performed at 300K with N^+ ions of energy 5 keV (dose of 1.5×10^{13} cm^{-2}), 20 keV (dose of 5×10^{13} cm^{-2}) plus 50 keV (dose of 1.3×10^{14} cm^{-2}) and 130 keV (dose of 3.5×10^{14} cm^{-2}), followed by rapid thermal annealing (RTA) for 2 mins under a flowing O_2 ambient. We also annealed some of the samples in either a conventional tube furnace or a pulsed laser deposition chamber under O_2 ambients for 45 mins, with the same basic trends observed in diode behavior as for the RTA processed devices. The backside of the substrates was deposited with full area contacts of e-beam deposited Ti (20 nm)/Au (200nm) annealed at 400°C Circular front-side contacts of Ni (20nm)/Au (80nm) with